

**Solid Mechanics Report:  
PMMA Strength Characteristics**

MAE 171A

Professors Jan Kleissl, Marko Lubarda, Alessandro Marinoni



**Team Members**

Ravi Harun  
Rayyan Khalid  
Alice Khalil  
Tanmay Prakash

## I. ABSTRACT

In this study, we explored and characterized the relationships between solid mechanics concepts by conducting tensile tests on Polymethylmethacrylate (PMMA) dogbone specimens. Using a tensile testing machine, we measured the force exerted to enable 2 mm elongation per minute until failure and buckling in different iterations to determine stress and strain, allowing us to begin to analyze the impact of cross-sectional design variations on the effective elastic modulus and ultimate strength of the specimen. Doing so allowed us to identify tactics to maximize ultimate strength and effective elastic modulus, which is significant for optimizing materials. Our results demonstrated that reducing material symmetrically or having a hexagonal pattern within the specimen decreased the overall effective density relative to the bulk material. Experimental results contradicted our assumption of increased ultimate strength and effective elastic modulus. This study provides significant insight into optimizing material performance and showcases the significance of tensile testing for data collection and analysis.

## II. INTRODUCTION

In the field of material science, the mechanical characterization of polymers plays a crucial role in applications ranging from construction to biomedical devices. This report focuses on Polymethylmethacrylate (PMMA), a widely used acrylic material known for its strength and clarity [3]. The primary objective of this experiment is to determine the tensile elastic and failure properties of PMMA and use this data to design a quasi-two-dimensional structured material aimed at achieving high strength and modulus to effective density ratios at low densities.

Recent advancements in material testing, such as the application of universal testing systems and digital image correlation, allow for precise measurement of material properties under various conditions. This experiment aims to harness these technologies to explore the mechanical behavior of PMMA, specifically its stress-strain relationship, elastic modulus, and yield strength, as per ASTM standards.

Significant research has been conducted on PMMA, highlighting its versatile applications and the importance of understanding its mechanical properties under different loading conditions. For instance, Zheng et al. (2014) [1] and ASTM standard D638-22 [2] have provided foundational insights into the mechanical testing of plastics, which guide our experimental methodology.

The hypothesis posits that the structured design of PMMA can be optimized to enhance its mechanical performance while maintaining a lower effective density compared to bulk material. This will be tested through a series of tensile tests and analyzed using DICe - Digital Image Correlation Engine - to obtain accurate strain measurements. The results will not only contribute to a better understanding of PMMA's mechanical properties but also assist in the material selection process for engineering applications where weight and strength are critical factors.

## III. PROCEDURES

In our lab, we conducted a series of tensile tests on acrylic (PMMA) using the Instron® 3400 Series Universal Testing System equipped with a 2530 Series High Force Load Cell and Manual Wedge Action Grips. The PMMA specimens were prepared to meet the ASTM D638-22 standards, shaped into dogbone geometries to ensure uniform stress distribution during testing. We marked the gauge lengths accurately with a marker and labeled each specimen for clarity during the testing process.

We then mounted the specimens securely using the manual wedge action grips, which provides a self-tightening feature that increases grip as the load increases, minimizing the risk of slippage. The setup included a 2530 Series High Force Load Cell, known for its precision and overload protection, ensuring the accuracy and safety of our tests.

The test sequence was controlled through the Bluehill Universal software, where we set the necessary parameters such as the speed of the test and the expected range of force which we applied at 2mm/min. As the machine applied tension to each specimen, real-time data on force and displacement were recorded. Concurrently, a camera was used to record the deformation of each specimen (taken every 10 seconds until failure) to be used later for the Digital Image Correlation engine (DICe). This allowed us to visualize and measure strain distribution and detect any concentration points or irregularities in the material's deformation.

After testing, we analyzed the data to calculate the material's mechanical properties, such as elastic modulus, yield strength, and ultimate tensile strength. The DIC software facilitated the processing of images to extract quantitative strain data, enabling a comprehensive analysis of the material's behavior under stress. The integration of mechanical testing with digital image analysis provided a robust framework for understanding the mechanical properties of PMMA, ensuring its optimal use in various applications.

#### IV. RESULTS

We will investigate quasi-two-dimensional structured materials and the mechanical characterization of their tensile elastic and failure properties. Using PMMA as the material and the Instron® 3400 Series Universal Testing System for tensile testing, the experiments were structured to explore the relationship between effective density, strength, and elastic modulus. The testing sequence began with a solid PMMA specimen loaded to failure, followed by a solid PMMA specimen subjected to a maximum of 6 mm of displacement until returning to 50% of its maximum load, finally, a customized design of a geometric-distribution altered PMMA with lowered overall effective density.

##### IV.1. Dogbone Specimen Loaded to Failure

In our initial series of tensile tests, we examined the mechanical behavior of a standard dogbone-shaped specimen under uniaxial tensile stress. The stress versus strain curve for this specimen [Fig 1.1], provides a clear representation of the material's response to applied forces. The test was conducted under controlled conditions to minimize any external factors influencing the material properties.

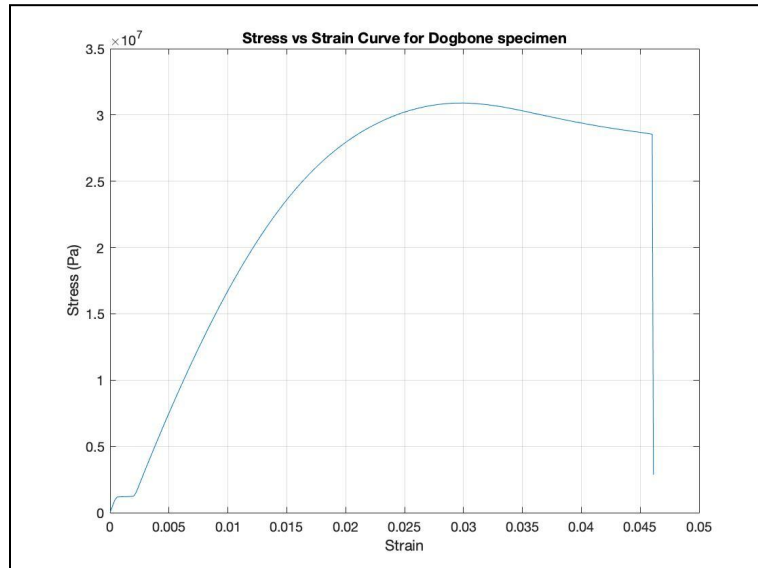


**Figure 1.1:** Stress-strain relationship of a Dogbone Specimen loaded to failure. The curve begins with a linear elastic region. As the strain increases, the material enters a plastic region before reaching its ultimate tensile strength, and eventually, failure.

The curve demonstrates an initial elastic region where the stress increases linearly with strain, reflecting the material's elastic deformation. The linear portion of the curve, indicative of the material obeying Hooke's Law, extends until a strain of approximately 0.01, which marks the transition from the elastic to plastic deformation. This yield point is characterized by a noticeable deviation from the initial straight line in the stress-strain curve. The yield strength measured for this test is approximately 1.2 MPa and the elastic modulus is approximately 1.96 GPa.

Following the yield point, the curve flattens slightly, suggesting a reduction in the material's stiffness. This portion of the curve typically indicates a hardening phase where the material can still bear load but with less stiffness compared to the elastic phase. The hardening continues until the ultimate tensile strength of 30.9 MPa is reached, which represents the maximum stress the material can sustain.

The ultimate tensile strength is observed at a strain of approximately 0.035, beyond which the material began to neck and eventually failed. The stress then sharply decreases as the specimen undergoes necking, leading to failure at a higher strain, underscoring the ductility of the PMMA material in accommodating significant deformation beyond the yield point before failure.

The stress-strain curve concludes with the fracture of the specimen, marking the end of the test [Fig 1.1]. The total area under the curve up to the point of fracture provides an estimate of the material's toughness, indicating the amount of energy it absorbed during the test.

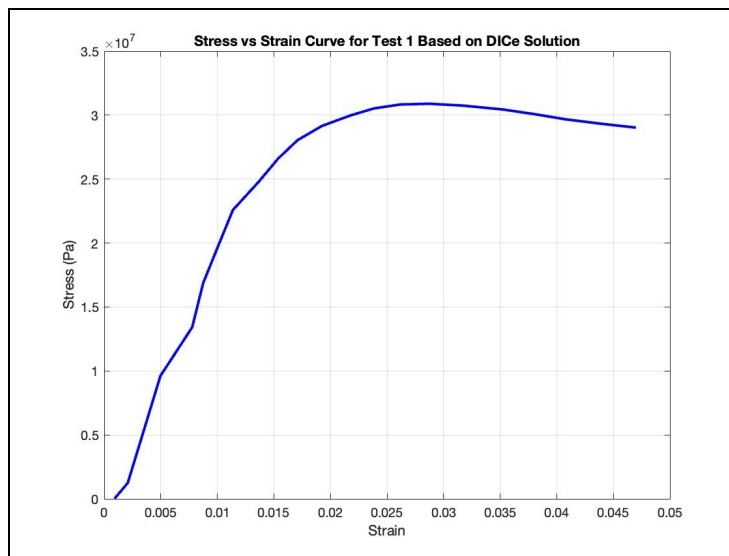


**Figure 1.2:** Stress-strain relationship of a Dogbone Specimen loaded to failure obtained from Digital Image Correlation engine (DICe) solution analyzing 23 images from 1 reference image.

Lastly, further imaging analysis using the DICe software poised similar results to the stress-strain curve seen in [Fig 1.1]. For this first test, there were 24 images taken until the end of the experiment, with the region of interest specified [A1] to measure the yy-displacement. The resulting stress strain-curve is seen in [Fig 1.2] with a UTS of 30.89 MPa at strain 0.019 strain obtained via MATLAB.

## IV.2. Dogbone Specimen Subjected to 6 mm Displacement

In our second series of experiments, we examined the mechanical behavior of an identical dogbone-shaped specimen under uniaxial tensile stress as before. In this test however, the specimen was loaded until it reached approximately 6 mm of displacement before being unloaded to 50% of its maximum load. This reduction in load led to corresponding decrease in stress, effectively illustrating the material's response under reverse loading conditions.



**Figure 1.3:** Stress-strain relationship of a Dogbone Specimen loaded to 6mm displacement, then returned to 50% of maximum load. The curve begins with a linear elastic region. As the strain increases, the material enters a plastic region before reaching its ultimate tensile strength, and eventually, takes a sharp inward curve.

The stress versus strain curve for this specimen [Fig 1.3], displays the material's response to the unique applied forces. After reaching the 6 mm displacement, the curve exhibits a sharp inwards turn, representing the unloading phase and its effect on the material.

Once again, the curve initially illustrates an elastic region characterized by the linear increase in stress and strain, thereby indicating the material's accordance with Hooke's Law. This linear trend extends to approximately 0.01 strain. The elastic modulus measured was approximately 1.87 GPa, slightly lower than in the initial full-load test.

The yield strength observed through this test is approximately 1.21 MPa. This value is critical for understanding at what stress level the material will begin to undergo permanent changes in its structure in response to applied forces.

The ultimate tensile strength (UTS), the maximum stress the material could withstand before failing, was recorded at approximately 30.77 MPa which happens at 0.032 strain. This value was reached right before the controlled unloading began, representing the peak load capacity of the material under the specified test conditions.

Furthermore, the stress decreased linearly as the load was reduced, following a similar but not identical path to the initial loading phase. This behavior highlights the material's viscoelastic characteristics, where the path of unloading does not exactly mirror the loading path due to the time-dependent mechanical response of the material. The elastic modulus calculated from the unloading

phase was slightly lower than that from the loading phase, indicating a change in the material stiffness after being subjected to significant strain.

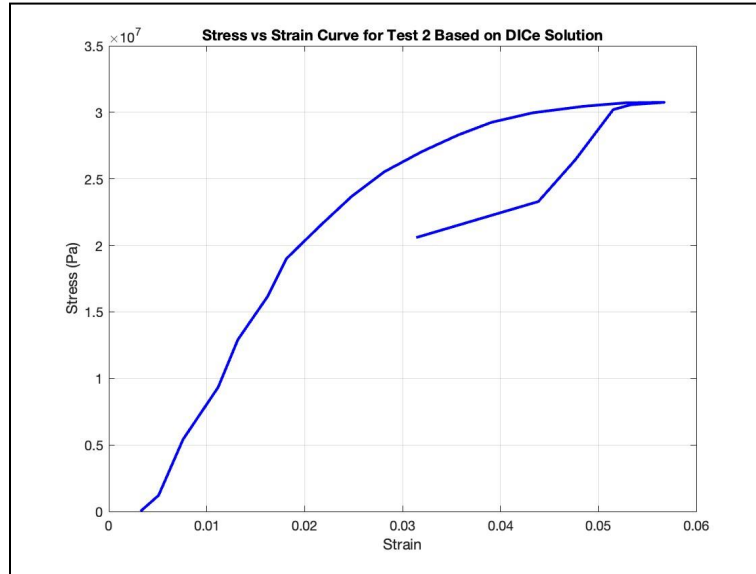


**Figure 1.4:** Stress-strain relationship of a Dogbone Specimen loaded to 6mm displacement obtained from Digital Image Correlation engine (DICe) solution analyzing 22 images from 1 reference image.

Lastly, further imaging analysis using the DICe software poised similar results to the stress-strain curve seen in [Fig 1.3]. For this second test, there were 24 images taken until the end of the experiment, with the region of interest specified [A1] to measure the yy-displacement. The resulting stress strain-curve is seen in [Fig 1.4] with a UTS of 30.75 MPa at strain 0.0568 strain obtained via MATLAB.

### IV.3 Customized Design of Dogbone Specimen

In our third series of tensile tests, we examined the mechanical behavior of a modified PMMA dogbone specimen that featured a custom design along its central perpendicular axes of symmetry [A2]. Our objective was to maximize the effective elastic modulus and ultimate strength while having a effective density no more than 30% of the original bulk acrylic. The design aimed to utilize the mechanical advantages of geometric distribution to improve material efficiency without compromising its strength. The resulting stress versus strain curve portrays the material's response to applied forces until failure [Fig 1.5]. The test conditions were controlled.

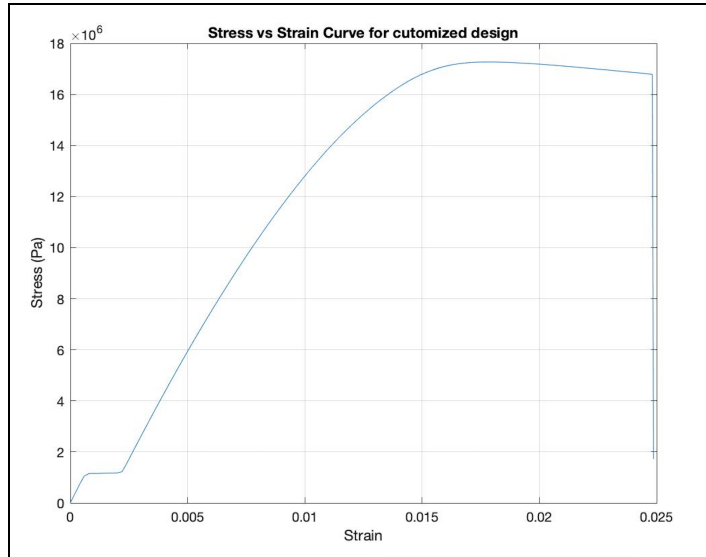


**Figure 1.5:** Stress-strain relationship of a Customized Design Dogbone Specimen loaded to failure. The curve begins with a linear elastic region. As the strain increases, the material enters a plastic region before reaching its ultimate tensile strength, and eventually, failure.

Consistent with the earlier two sections, the curve initially portrays an elastic region with a linear increase of stress and strain - compliant with Hooke's Law. This elastic behavior continues until approximately 0.01 strain.

The values obtained from MATLAB for the mechanical properties are as follows:

- Elastic Modulus: 1.5 GPa
- Yield Strength: 1.18 MPa
- Ultimate Tensile Strength: 17.27 MPa

These values indicate that, although the design effectively reduced the material's overall effective density, it did not succeed in enhancing the mechanical properties as anticipated. The elastic modulus and the ultimate tensile strength were both lower compared to the original dogbone specimen. This reduction in mechanical properties can be attributed to decreased material volume. Despite the strategic placement and orientation of the cut-outs, which were intended to enhance load-bearing efficiency by redirecting stress flow through optimized paths, the significant reduction in material ultimately compromised the specimen's ability to withstand stress.

Additionally, the introduction of geometric cut-outs in the design likely increased stress concentration at the edges of these hexagonal features. Stress concentration occurs when changes in geometry lead to localized increase in stress. In this specimen, each cut-out acts as a potential site for stress concentration, particularly under tensile loading. This phenomenon can significantly weaken the overall structural integrity by focusing stress in smaller areas, which may lead to premature failure even if the total applied load is within the material's theoretical strength capacity.

The presence of stress concentrations, therefore, might have contributed substantially to the lower ultimate tensile strength observed in the customized design compared to the standard dogbone specimen. This suggests that while the design aimed to optimize material usage and maintain strength through

strategic material removal, the resultant increase in stress concentration undermined these benefits, leading to reduced performance.

Further insight into the mechanical behavior of the customized dogbone specimen was gained through finite element analysis (FEA) conducted using ANSYS. The simulations provided detailed visualizations of the stress distribution and deformation under applied loads, which are crucial for understanding the stress concentration effects introduced by the geometric modifications.

The FEA results revealed significant stress concentration around the geometric cut-outs, particularly where the material transitioned from the solid areas into the voids [Fig 1.6]. These stress concentrations are likely contributors to the specimen's reduced mechanical performance observed during the physical tests. The highest stress regions, indicated by the red and yellow zones in the simulation, correspond to areas where failure is most likely to initiate under continued loading.

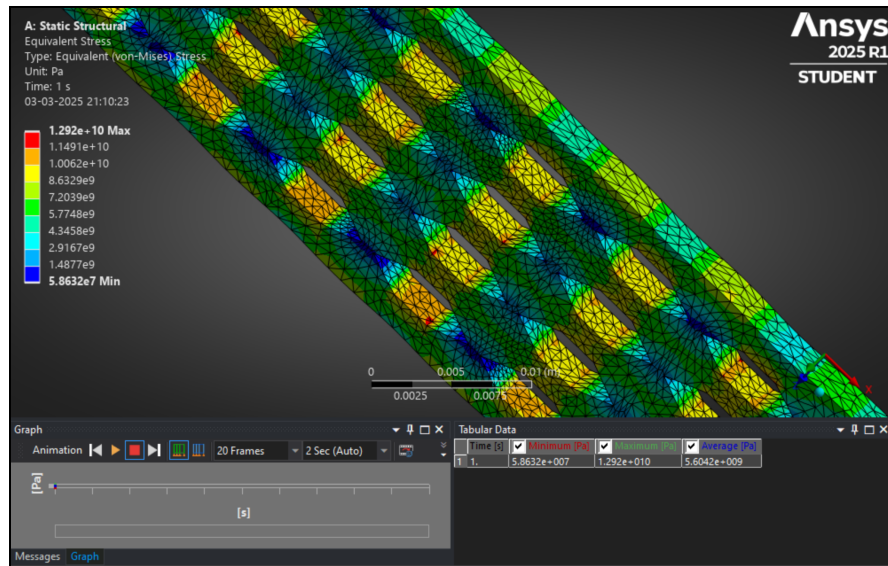


**Figure 1.6:** ANSYS FEA Simulation portraying the customized design of the PMMA dogbone specimen and the significant stress concentrations around each of the cut-outs.

Additionally, the analysis highlighted the deformation behavior of the specimen. The total deformation visualized across the specimen demonstrated how the material responded to tensile forces, with maximum deformation occurring near the center of the length, aligning with the areas of greatest material removal. This deformation pattern supports the observed mechanical test results where the material exhibited lower stiffness and strength compared to the original design.

## V. DISCUSSION

The results obtained from the solid mechanics and tensile testing provided valuable insights into the relationship between geometric distribution and material properties, particularly how effective density affects elastic modulus and ultimate tensile strength. After designing a customized PMMA dogbone, the tensile-tests portrayed that while effective density was successfully reduced, it also exhibited a decrease in both elastic modulus and ultimate tensile strength - an unexpected outcome. The summary of our results are tabulated below in table 1.

Table 1: Summary of the results

Type	UTS [MPa]	Yield Strength [MPa]	Young's Modulus [GPa]
Dogbone until failure	30.9	1.2	1.96
Dogbone until 6mm displacement	30.77	1.21	1.87
Dogbone with customized design	17.27	1.18	1.5

The Instron® 3400 Series Universal Testing System allowed for clear visualizations and plots of the PMMA dogbones' mechanical behavior under specific loads. By analyzing the responses of both the original and altered specimen, it became evident that the new geometric distribution and effective density reduction significantly influenced the material performance. The existence of geometric cut-outs led to stress concentrations, contributing to a decrease in elastic modulus and ultimate tensile strength.

Table 2: Comparison of UTS and their strain values between alongside their errors

Type	UTS [MPa]			Strain at UTS		
	Obtained via Experiment	Obtained via DICe	Error	Obtained via Experiment	Obtained via DICe	Error
Dogbone until failure	30.90	30.89	0.03%	0.035	0.019	45.71%
Dogbone until 6mm displacement	30.77	30.75	0.06%	0.032	0.0568	77.5%

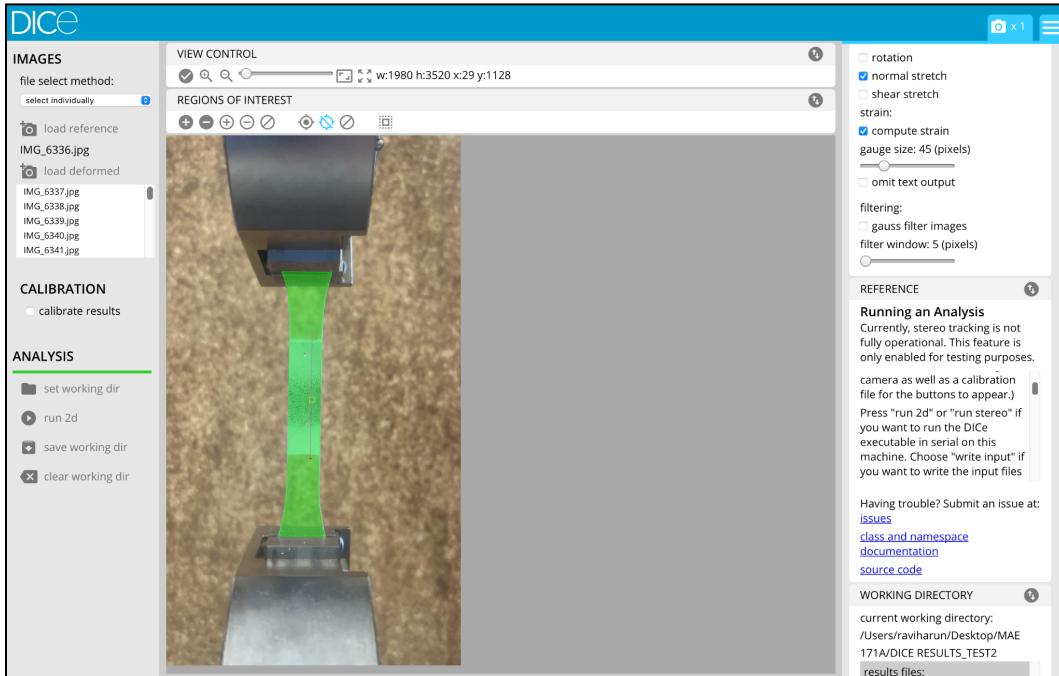
Table 2 shows an error of several between the experimentally obtained Ultimate Tensile Strength (UTS) values and the strain in which UTS occurs and the values obtained in the DICe. In particular the errors for the ultimate tensile strength are relatively small compared to that of their strains. This is because the stress for experiment and DICe is the same, due to the DICe being unable to measure force visually. However, we utilized the DICe mainly to obtain the y-strain of the images of the dogbone that we took. We believe that a large error between the experimentally obtained strain at UTS and that of DICe may have been caused by the DICe's surface imaging methods, which might have inconsistencies with its resolution, calibration and surface conditions.

Future iterations of this design could benefit from a more detailed analysis of stress distribution using finite element analysis (FEA) to identify and mitigate high-stress regions. Adjustments may include optimizing the shape and size of the cut-outs or reconfiguring their layout to distribute stress more evenly across the specimen. This approach would aim to reduce the negative impact of stress concentrators while still achieving the desired reduction in material effective density.

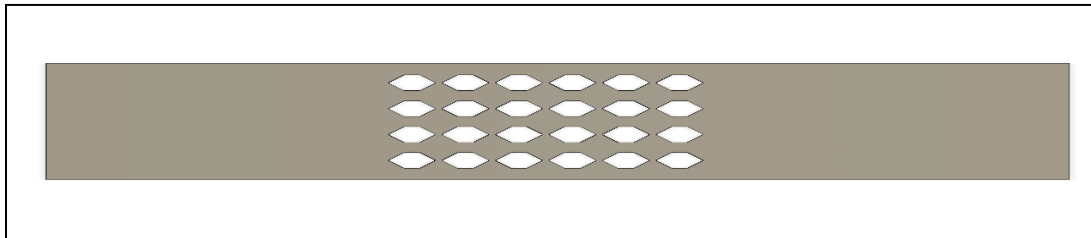
## REFERENCES

- [1] Zheng, X., et al. "Ultralight, ultrastiff mechanical metamaterials." *Science*, vol. 344, no. 6190, 2014, pp. 1373-1377. DOI: 10.1126/science.1252291.
- [2] ASTM International. "Standard Test Method for Tensile Properties of Plastics." ASTM D638-22, West Conshohocken, PA: ASTM International, 2022. Web.  
<https://www.astm.org/DATABASE.CART/HISTORICAL/D638-22.htm>.
- [3] Harper, Charles A. "Handbook of Plastics, Elastomers, and Composites." 4th Ed., McGraw-Hill, 2002.
- [4] ANSYS, Inc. (2023). ANSYS Fluent (Version 2023 R1). <https://www.ansys.com>

## APPENDIX



[A1]: Console view of Digital Image Correlation engine (DICe) for the second test of dogbone specimen, displaying region of interest (green) with active lines (red) and points (purple).



[A2]: CAD image of the customized design of the PMMA dogbone specimen.

Data Sources

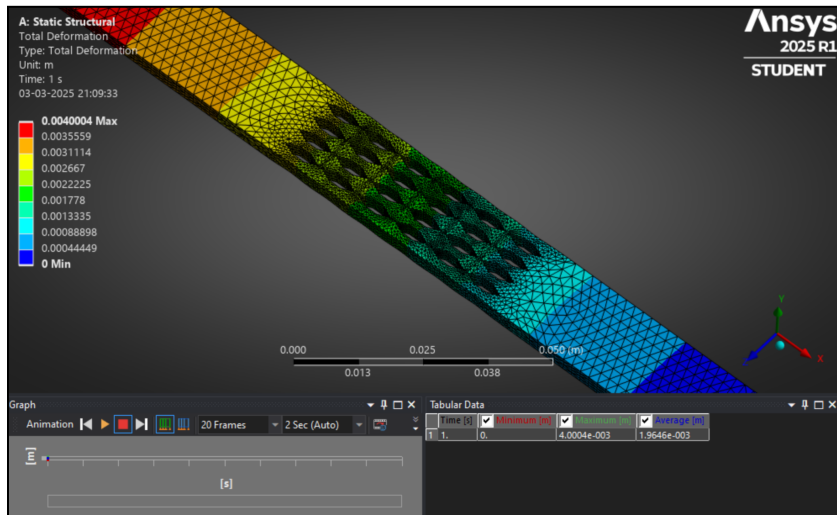
	A	B	C	D	E
1	Contents of Engineering Data				Description
2	Material				
3	ACRYLIC				Fatigue Data at zero mean stress comes from 1998 ASME BPV Code, Section 8, Div 2, Table 5 -110.1
4	Structural Steel				
*	Click here to add a new material				

Properties of Outline Row 3: ACRYLIC

	A	B	C	D	E
1	Property	Value	Unit		
2		Table			
3		1180	kg m <sup>-3</sup>		
4					
5	Derive from	Young's Modulu...			
6	Young's Modulus	3.2	GPa		
7	Poisson's Ratio	0.35			
8	Bulk Modulus	3.5556E+09	Pa		
9	Shear Modulus	1.1852E+09	Pa		
10		66	MPa		
11		55.158	MPa		

[A3]: Image of our acrylic material properties on ANSYS



[A4]: Image of static structural analysis results in ANSYS (Isometric view)

**Individual Contributions:**

**Alice:** Wrote abstract section, wrote discussion section, wrote parts of results section. Also created figure descriptions in text-citations.

**Tanmay:** Ansys Simulations (Stati Structural and Explicit Dynamics), abstract, introduction, results, editing all sections, proof-reading.

**Ravi:** Did imaging analysis using DICe, reported DICe results and conducted error analysis in the Discussion section. Formatted the report and created figure descriptions for several figures and appendices.

**Rayyan:** Wrote Introduction and Procedures section, parts of Results section, table in the discussion section, and graphs in the results section.